JOURNAL OF AGRICULTURAL AND FOOD CHEMISTRY

Article

pubs.acs.org/JAFC

Mycosporine-like Amino Acids and Other Phytochemicals Directly Detected by High-Resolution NMR on Klamath (*Aphanizomenon flos-aquae*) Blue-Green Algae

Valeria Righi,[†] Francesca Parenti,[‡] Luisa Schenetti,[#] and Adele Mucci*[,‡]

[†]Dipartimento di Scienze per la Qualità della Vita, Università di Bologna, via Corso d'Augusto 237, 47921 Rimini, Italy

[‡]Dipartimento di Scienze Chimiche e Geologiche and [#]Dipartimento di Scienze della Vita, Università di Modena e Reggio Emilia, Via G. Campi 103, 41125 Modena, Italy

Supporting Information

ABSTRACT: This study describes for the first time the use of high-resolution nuclear magnetic resonance (NMR) on Klamath (*Aphanizomenon flos-aquae*, AFA) blue-green algae directly on powder suspension. These algae are considered to be a "superfood", due to their complete nutritional profile that has proved to have important therapeutic effects. The main advantage of NMR spectroscopy is that it permits the detection of a number of metabolites all at once. The Klamath alga metabolome was revealed to be quite complex, and the most peculiar phytochemicals that can be detected directly on algae by NMR are mycosporine-like amino acids (porphyra-334, P334; shinorine, Shi) and low molecular weight glycosides (glyceryl β-D-galactopyranoside, GalpG; glyceryl 6-amino-6-deoxy-α-D-glucopyranoside, ADG), all compounds with a high nutraceutical value. The presence of *cis*-3,4-DhLys was revealed for the first time. This molecule could be involved in the anticancer properties ascribed to AFA.

KEYWORDS: *Aphanizomenon flos-aquae, nuclear magnetic resonance spectroscopy, Klamath algae, mycosporine-like amino acids, glycosides, ESI-QTOF mass spectrometry*

INTRODUCTION

Aphanizomenon flos-aquae (AFA) is a wild freshwater unicellular microalga that spontaneously grows in copious amounts in Upper Klamath Lake (Klamath Falls, OR, USA), a volcanic lake with hot, deep, and mineral-rich waters. The combination of water properties, clean air, and high-intensity sunlight maked the unique ecosystem of Upper Klamath Lake the most perfect growing environment for this alga. AFA from Klamath Lake attracts the interest of several scientists owing to its complete nutritional profile and therapeutic properties, and it is consumed as a nutrient food source and for its health-enhancing properties.[1−5]

The microalga AFA Klamath exerts beneficial effects on various neurological dysfunctions, including neurodegenerative diseases such as Alzheimer's and Parkinson's, multiple sclerosis, hyperactivity and attention deficit disorders, autism, depression, memory deficit, and mood disturbances.[1,6−12]

AFA algae are prokaryote cells (cyanobacteria), which are capable of implementing the photosynthesis process despite their simple structure. Their green-blue color is due to the presence of phycobiliproteins, a family of highly soluble and reasonably stable fluorescent proteins containing a covalently linked tetrapyrrole prosthetic group (phycocyanobiline). Phycocyanobilines are pigments that collect light and convey it (through fluorescence resonance energy transfer) to a pair of chlorophyll molecules located in the photosynthetic reaction center of the cyanobacteria, starting the photosynthetic process. AFA is an important source of the blue photosynthetic pigment phycocyanin (a complex between the pigment phycocyanobiline with phycobiliproteins), which has been described as a strong antioxidant[13−15] and anti-inflammatory[16,17] natural compound, as evidenced by in vitro and in vivo studies on phycocyanin from the cyanophyta *Spirulina platensis*. In addition, AFA Klamath is an important source of β-phenylethylamine, a sort of natural endogenous amphetamine-like compound that is able to modulate mood.

Recently, attention has also been devoted to the composition of AFA, which appears to contain mycosporine-like amino acids (MAAs), in particular porphyra-334 (P334) and shinorine (Shi), as monoamine oxidase (MAO) inhibitors, which seem present in relatively high concentration in AFA Klamath microalgae.[5,18,19] These are structurally simple water-soluble molecules, with a molecular weight of 300−350 Da, that easily cross the blood−brain barrier and then are able to express their MAO-B inhibitory potential in the area where it is mostly needed, the brain. Moreover, MAAs are reported to be antioxidant, UV-protective, and wound-healing agents.[20]

For the chemical analysis of these biologically active compounds, different conventional techniques are used: extraction, chromatography,[21−23] UV−vis and IR.[24,25] Each of these chemical analysis techniques allows identifying only one or a few classes of chemical compounds at a time and requires a sample pretreatment.

In this work, we present, for the first time to the best of our knowledge, the application of high-resolution nuclear magnetic

Received: June 10, 2016
Revised: August 5, 2016
Accepted: August 18, 2016
Published: August 18, 2016

DOI: 10.1021/acs.jafc.6b02615
J. Agric. Food Chem. 2016, 64, 6708−6715

Scheme 1. Structures of Porphyra-334 (P334), Shinorine (Shi), Glyceryl β-D-Galactopyranoside (GalpG), *cis*-3,4-Dehydrolysine (DhLys), and Glyceryl 6-Amino-6-deoxy-α-D-glucopyranoside (ADG)

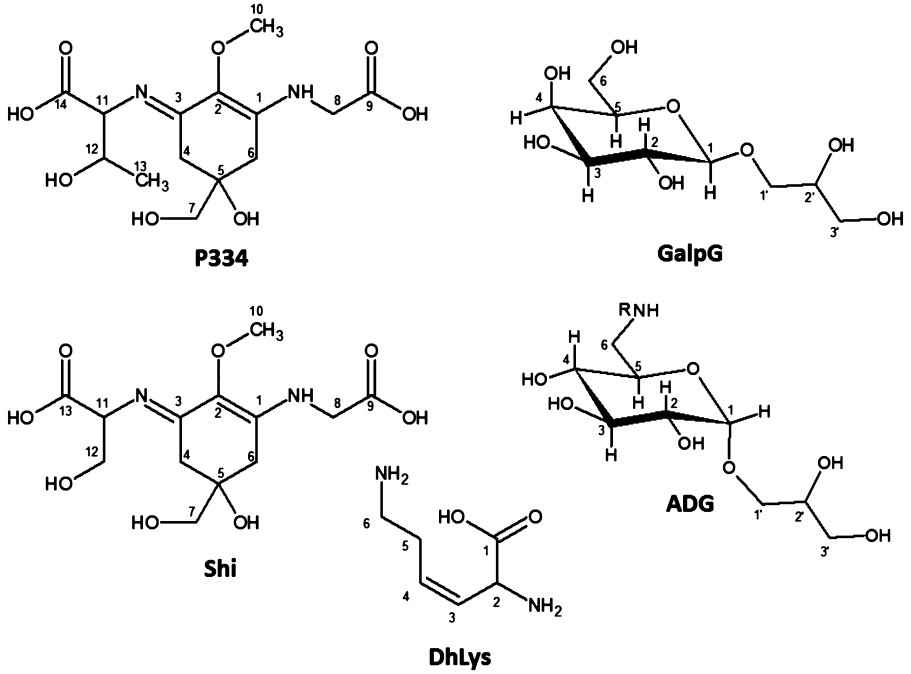

resonance (NMR) spectroscopy to the study of deuterated water (D_2O) suspensions of commercially available Klamath powder for the detection of several metabolites all at once. This approach has the advantage of avoiding any sample pretreatment that can alter alga composition. The NMR spectra obtained are very complex, and this work does not expect to be exhaustive in describing the metabolome of AFA but, despite the evident spectral overcrowding, we will show that P334, and to a minor extent Shi, can be detected directly in the water suspension, without the need for extraction. Together with these MAAs, another two molecules were recognized (Scheme 1), glyceryl β-D-galactopyranoside (GalpG) and *cis*-3,4-dehydrolysine (DhLys) among other minor species. These findings were checked with electrospray ionization quadrupole-time-of-flight mass spectrometry (ESI-QTOF-MS) and low-energy collision-induced dissociation tandem mass spectrometry (CID MS/MS).

MATERIALS AND METHODS

Sample Preparation. A suspension of dry powder of alga Klamath (Farmalabor S.r.l, Canosa di Puglia, Italy, batch P1001594-000), 40 mg in 700 μL of D_2O 99.8%, was sonicated at 25 °C for 1 h and directly used for NMR measurements. Samples for ESI-QTOF-MS measurements were obtained by suspending algae in deionized water (1 mg in 1 mL), sonicated at 25 °C for 1 h, centrifuged at 13000 rpm, for 10 min, and the surnatants, diluted 1:30 in deionized water, were directly analyzed. All measurements were performed at autogenous pH (5.6).

NMR Experiments. NMR spectra were recorded with an AVANCE III HD 600 spectrometer (Bruker) equipped with a CryoProbe BBO H&F 5 mm (operating at 600.13 and 150.90 MHz for proton and carbon, respectively) at 300 K. Ala CH_3 signal (at 1.47 and 19.0 ppm, for proton and carbon, respectively, see Table S1) was used as internal reference for ^1H and ^{13}C chemical shifts. 1D proton spectra were acquired using the standard zgcppr sequence with 2.5 s water presaturation during relaxation delay, 12 kHz spectral width, 64k data points, and 64 scans. 2D COSY spectra were acquired using a standard pulse sequence (cosygpprqf) and 1 s water presaturation during relaxation delay, 7 kHz spectral width, 4k data points, 16 scans per increment, and 512 increments. 2D TOCSY spectra were acquired using a standard pulse sequence (mlevgpph19) and 0.5 s relaxation delay, 100 ms mixing (spin-lock) time, 7 kHz spectral width, 4k data points, 32 scans per increment, and 512 increments. 2D NOESY and ROESY spectra were acquired using standard pulse sequences (noesygpph19, roesyphpr) and 1 s relaxation delay, 500 and 250 ms mixing time, respectively, 7.2 kHz spectral width, 4k data points, 24 scans per increment, and 512 increments. 2D HSQC edited spectra were acquired using a standard pulse sequence echo-antiecho phase sensitive (hsqcedetgpsp.3) and 0.5 s relaxation delay, 1.725 ms evolution time, 7 kHz spectral width in f_2, 4k data points, 96 scans per increment, 25 kHz spectral width in f_1, and 320 increments. 2D HMBC spectra were acquired using a standard pulse sequence (hmbcgplpndqf) with 0.5 s relaxation delay, 3.4 ms low-pass J filter and 50 ms evolution time, 7 kHz spectral width in f_2, 4k data points, 128 scans per increment, 30 kHz spectral width in f_1, and 300 increments. An HSQC-TOCSY experiment was acquired using a standard pulse sequence (hsqcdiedetgpsisp.1) and 0.5 s relaxation delay, 1.725 ms evolution time, 110 ms spin-lock, 8 kHz spectral width in f_2, 2k data points, 96 scans per increment, 23 kHz spectral width in f_1, and 280 increments.

ESI-QTOF Experiments. Positive and negative ion high-resolution ESI-QTOF-MS and low-energy CID MS/MS spectra were acquired with an 6520 Accurate-Mass QTOF LC-MS (Agilent Technologies) coupled with a HPLC Agilent series 1200 equipped with a Zorbax SB-C18 column, 100 × 2.1 mm i.d., 3.5 μm particle size (Agilent). Eluents were acetonitrile (eluent A) and H_2O with 0.2% ammonium formate (eluent B). Chromatographic runs were performed using a gradient of eluent A [starting from 1% (1 min) to 40% (in 20 min) to 100% (in 10 min)]. The solvent flow rate was 0.3 mL/min, the temperature was kept at 25 °C, and the injector volume selected was 2 μL. Total ion current (TIC) chromatograms were acquired in the mass range between m/z 50 and 1700. Nitrogen was used as collision gas in MS/MS experiments. Nitrogen nebulizer pressure was 30 psi, nitrogen dry gas flow and temperature were 9 L/min and 350 °C, respectively, and capillary voltage was 3.5 kV. Exact masses were checked to verify the correspondence to the proposed molecular formulas, within 10 ppm that is the maximum estimated mass error. The isotopic peak intensity ratios of molecular species where checked with the "generate-formula-

DOI: 10.1021/acs.jafc.6b02615
J. Agric. Food Chem. 2016, 64, 6708−6715

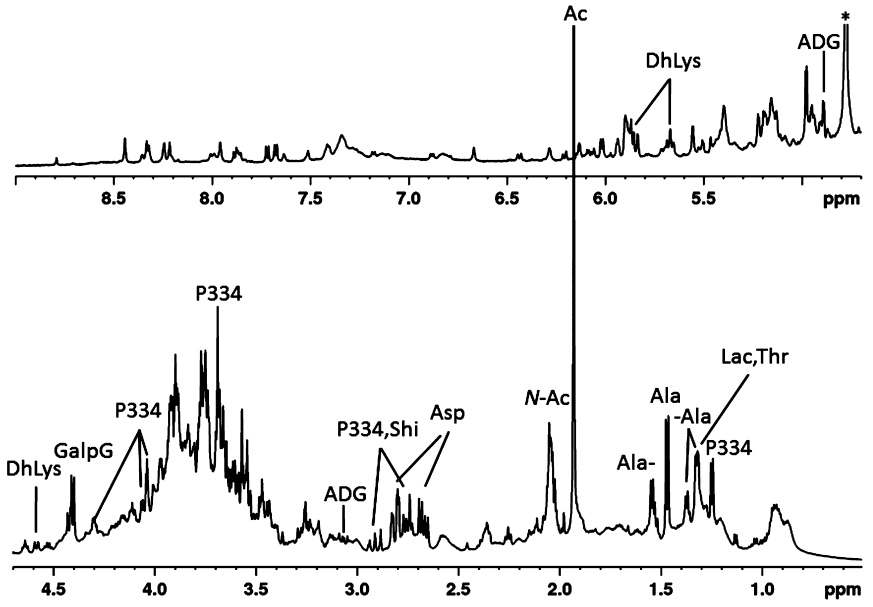

Figure 1. Water-presaturated ^{1}H NMR spectrum of Klamath alga suspension in D_2O. * residual HDO signal. Interesting metabolites are labeled: porphyra-334 (P334), shinorine (Shi), glyceryl β-D-galactopyranoside (GalpG), *cis*-3,4-dehydrolysine (DhLys), glyceryl 6-amino-6-deoxy-α-D-glucopyranoside (ADG), alanine and bound forms of alanine (Ala, Ala-, and -Ala), acetate (Ac), *N*-acetyls (*N*-Ac), lactate (Lac), aspartate (Asp), threonine (Thr).

from-peaks" tool of Qualitative Analysis (version B.04.00, Agilent Technologies, Inc., 2011).

RESULTS AND DISCUSSION

Because powdered alga Klamath forms suspensions in D_2O, we first evaluated the use of high-resolution magic angle spinning (HR-MAS), which is an NMR technique that bridges the divide between high-resolution NMR in solution and solid-state NMR. HR-MAS is the preferred NMR technique when semisolid samples, such as vegetable tissues, are investigated. In fact, it does not need any pretreatment, extraction, or separation, and the signals from polar and apolar fractions are detected simultaneously.[26,27] Nevertheless, when the NMR AFA spectra obtained with HR-MAS probe were compared to those acquired with probes for liquids (AFA suspended into standard 5 mm NMR tubes), we did not observe any difference (Figure S1). Hence, we decided to carry out this investigation directly in this last way, that is, on suspensions of dry powder of alga Klamath in D_2O. The signals thus observed are due to molecules in solution, and the little suspended material does not affect negatively spectral resolution.

The water-presaturated ^{1}H NMR spectrum of alga Klamath suspension is reported in Figure 1. It is a very complex spectrum, dominated by the acetate signal at 1.93 ppm and then by signals within the carbohydrate region (5.5−3 ppm), the majority of which belong to high molecular weight species, which are in the negative NOE regime.[28]

Resonances due to aliphatic amino acids at low parts per million are also clearly detected. Lower signals are found in the anomeric/ethylenic region and very low resonances in the aromatic one. An attempt to disentangle, at least partially, this heavily overlapped pattern was done through 2D homonuclear and heteronuclear spectra. COSY, TOCSY, NOESY, ROESY, HSQC, HSQC-TOCSY, and HMBC spectra were acquired and analyzed, and a number of metabolites were identified. The results are reported in Tables 1 and S1.

Some of the detected metabolites (alanine, Ala; and other aliphatic amino acids, acetate, Ac; lactate, Lac; aspartate, Asp; glutamate, Glu; glutamine, Gln; threonine, Thr; glucose, Glc; etc.) are quite common in natural matrixes, and their signals can be readily interpreted and assigned. Nevertheless, in the case of alga Klamath a group of signals in the region 2.6−2.9 ppm, partially overlapping those of CH_2-β of Asp (H/C correlations: 2.82,2.68/39.7), attracted our attention. These resonances are due to two CH_2 with diastereotopic protons (H/C correlations: 2.89,2.74/36.1 ppm and 2.82,2.75/35.8 ppm, Figure 2), which give two AB systems. They also give H,C long-range correlations in HMBC spectrum (not shown) with carbons at 73.8, 128.0, 161.8, and 163.3 ppm, which allow assembly of the MAA skeleton (Scheme 1). This hypothesis was confirmed by other H,C long-range and H,H NOE and ROE correlations (Figure 3; Table 1) and allow the identification of the presence of P334. P334 should be in its protonated form, for both H-11 and H-8 give correlations with NH protons in TOCSY experiment. These data compare well with those reported in the literature.[18,29] Moreover, very close to P334 major signals, minor resonances were found at 2.92 and 2.77 ppm. They show clear ROESY cross peaks with protons at 4.34 and 3.57 ppm (Figure 3). The signal at 4.34 derives from a methine proton (C 63.3 ppm) that correlates in the COSY spectrum with methylene signals at 3.92 and 3.99 ppm (C 65.3 ppm) and with carbons at 177.5 and 161.9 ppm in the HSQC spectrum. This second set of minor signals was assigned to Shi, the other resonances of which overlap those of P334. Also in this case, the spectral data parallel those reported in the literature for Shi methyl ester.[30]

Due to the high overlapping of P334 and Shi signals in the ^{1}H NMR spectrum, an estimate of the relative P334/Shi molar ratio of about 3:1 is better obtained, in the hypothesis of a very similar conformation, from the integrals of the cross peaks between CH_2-4 and CH-11 in the ROESY spectrum. Alternatively, in the hypothesis of similar $^1J_{HC}$ coupling values for the C,H-11 pair in both compounds, the P334/Shi molar

DOI: 10.1021/acs.jafc.6b02615
J. Agric. Food Chem. 2016, 64, 6708−6715

Table 1. NMR Data (600 MHz, D_2O) for Selected Metabolites Found in AFA[a]

metabolite	nucleus	H (δ, ppm; J, Hz)	C (δ, ppm)	note[b]
P334	CH_2-8	4.03	49.5	HMBC 163.3 (C1), 177.7 (C9)
				COSY, TOCSY 8.6 (NH)
	CH_2-6	2.75 (d, J = 17.3), 2.82 (d, J = 17.3)	35.8	HMBC 163.3(C1)
				ROESY 4.03
	CH_2-7	3.57	70.4	HMBC 35.8, 36.1, 73.8 (C5)
	CH_2-4	2.89 (d, J = 17.3), 2.74 (d, J = 17.3)	36.1	HMBC 161.8 (C3), 73.8 (C5), 128.5 (C2)
				ROESY 4.06
	CH_3-10	3.69	62.2	HMBC 128.5 (C2)
	CH-11	4.06	67.3	HMBC 178.2 (C14), 161.8 (C3)
				TOCSY 7.63 (NH)
	CH_3-13	1.25 (d, J = 6.3)	22.2	HMBC 67.3, 71.0
				NOESY 2.89
				TOCSY 7.63 (NH)
	CH-12	4.30	71.0	COSY 1.25, 4.06
Shi serine residue	CH_2-4	2.92 (d, J = 17.2), 2.77 (d, J = 17.2)	36.1	ROESY 3.57, 4.34
	CH-11	4.34	63.3	HMBC 177.5 (C13), 161.9 (C3)
				COSY 3.92, 3.99
	CH_2-12	3.92 (t), 3.99 (d)	65.3	HMBC 177.5 (C13)
GalpG	CH-1	4.40 (d, J = 8)	105.9	ROESY 3.54, 3.65, 3.68 3.76, 3.91
	CH-2	3.55	73.7	HMBC 105.9, 75.5
	CH-3	3.65	75.5	HMBC 73.6
	CH-4	3.92	71.5	HMBC 78.0, 73.6, 75.5, 63.8
	CH-5	3.69	78.0	HMBC 63.8, 71.5
	CH_2-6	3.76, 3.79	63.8	HMBC 78.0
	CH_2-1′	3.76, 3.91	73.7	HMBC 105.9, 65.3
	CH-2′	3.93	73.2	HMBC 73.7
	CH_2-3′	3.60, 3.66	65.3	HMBC 73.7
ADG	CH-1	4.89 (d, J = 3.6)	101.1	HMBC: 70.9, 71.7, 75.9
				COSY 3.58
				TOCSY 3.07, 3.38, 3.26, 3.58, 3.75, 4.06
				ROESY 3.45, 3.58
	CH-2	3.58	74.4	
	CH-3	3.73 (t)	75.7	
	CH-4	3.26 (t, J = 13)	75.4	HMBC 54.9, 70.9, 75.7
	CH-5	4.05 (t, J = 10)	70.9	
	NCH_2-6	3.07 (dd, J = 9.7, 14.7), 3.38 (t, J = 14.7)	54.9	HMBC 70.9, 75.4
	CH_2-1′	3.45 (t), 3.94 (d)	71.7	HMBC 65.5, 73.6, 101.1
				TOCSY 3.69, 3.59, 3.94
				ROESY 3.45, 3.94
	CH-2′	nd	73.6	
	CH_2-3′	3.69, 3.59	65.5	
cis-3,4-DhLys	CH-2	4.59 (d, J = 9.8)	54.7	HMBC 128.1, 135.1, 175.6
				ROESY 2.66, 2.58
	CH-3	5.66 (t, J = 10.2)	128.1	
	CH-4	5.88 (m)	135.1	
	CH_2-5	2.58, 2.66	28.2	HMBC 135.1, 128.1, 41.3
	CH_2-6	3.13, 3.19	41.3	HMBC 135.1, 28.2

[a]Ala CH_3 signal (at 1.47 and 19.0 ppm, for proton and carbon, respectively, see Table S1) was used as internal reference for ^1H and ^{13}C chemical shifts. [b]Relevant correlations observed in 2D spectra: HMBC, TOCSY, COSY, ROESY, NOESY.

ratio can be estimated by the HSQC C,H-11 correlations (at 4.06/67.3 ppm for P334 and at 4.34/63.3 ppm for Shi) as 2.3:1. However, in this case, the volume of P334 C,H-11 cross peak is underestimated, due to its proximity to a CH_2 correlation of opposite sign.

The presence of both P334 and Shi was confirmed by ESI-MS and low-energy CID MS/MS spectra (see ESI-QTOF Experiments).

Another group of interesting and intense correlations was distinguished in the HSQC carbohydrate region. The most characteristic signals are the β-D-galactose doublet at 4.40 ppm

DOI: 10.1021/acs.jafc.6b02615
J. Agric. Food Chem. 2016, 64, 6708−6715

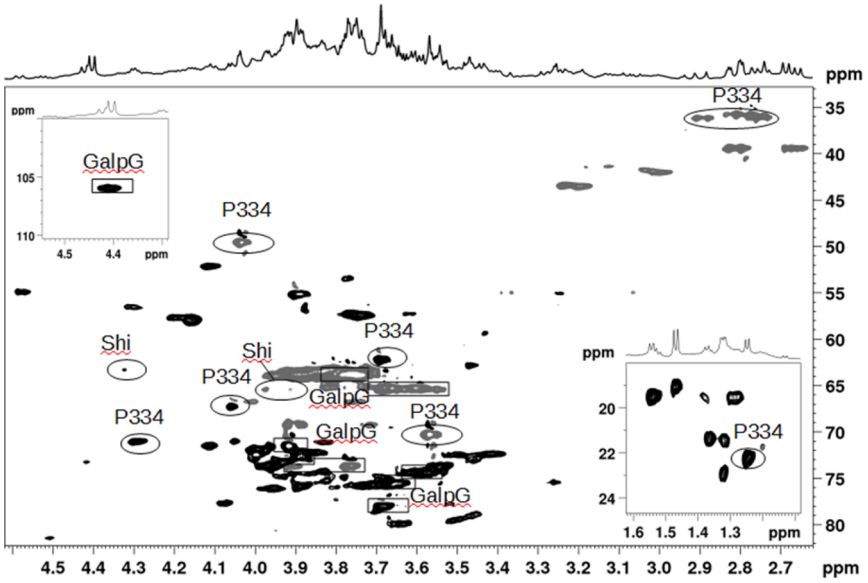

Figure 2. Partial HSQC spectrum of Klamath alga suspension in D_2O evidencing signals of P334, Shi (ovals), and GalpG (rectangles).

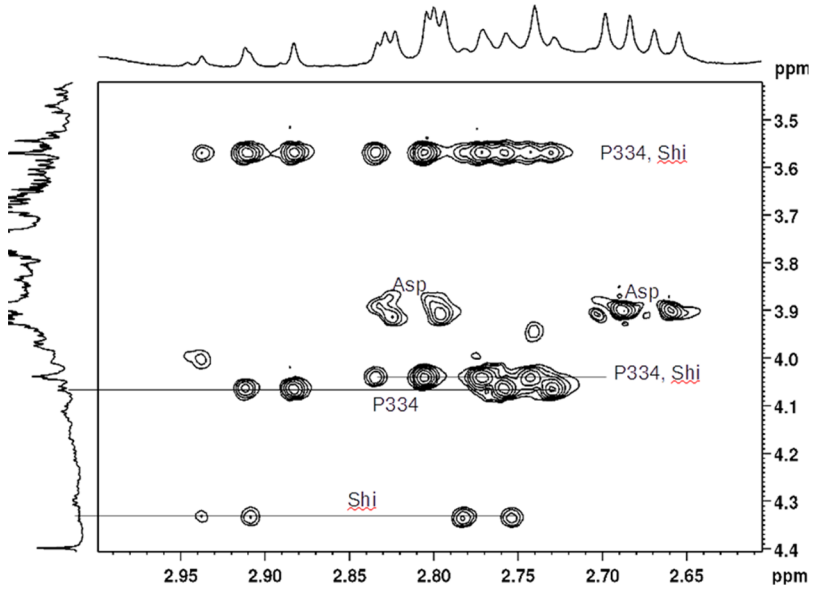

Figure 3. Partial ROESY spectrum of Klamath alga suspension in D_2O evidencing signals of P334 and Shi.

(bound to C at 105.8 ppm, which indicates the presence of a β-glycosidic linkage) and two methylene groups, with diastereotopic protons, and H,C correlations that are found at 3.76,3.91/73.7 and 3.60,3.66/65.3 ppm. Starting from the 4.40 doublet, it is possible to derive a β-galactose spin system, through COSY and TOCSY correlations, up to H-4 at 3.92 ppm, due to the low J coupling H-4,H-5 that lowers the efficiency of coherence transfer. Nevertheless, H-4 correlates with C-6, C-5, C-2, and C-3 in the HMBC spectrum, and these correlations permit reconstruction of the galactopyranosyl unit. Inter-residue ROE correlations between H-1 and 3.76, 3.91 methylene signals allow GalpG (Figure 2) to be recognized, and the HSQC-TOCSY spectrum (Figure S2a) confirms that 3.76, 3.91 protons belong to the same spin system to which 3.60, 3.66 protons belong, too. GalpG gives also rise to the highest signals in the ^{13}C spectrum, and its presence was confirmed by ESI-QTOF-MS results (see ESI-QTOF Experiments). This seems to us a quite peculiar finding, because α-D-galactopyranosyl glycerols are usually found in algae[31] and GalpG appears to be a glycoside that characterizes the AFA metabolome.

A minor doublet at 4.43 ppm (bound to C at 105.8 ppm) indicates the presence of another minor β-D-galactoside, the spin system of which was only partially identified. Similarly, other low correlations due to glycosidic units were found (Table S1). The presence of GalpG, and similar water-soluble molecules, could be related to different types of glycoglycerolipids[32] that have significant antitumor activities toward different targets.

Two interesting spin systems were also highlighted by TOCSY (Figure 4). The former recalls the spectral features of a 6-amino-6-deoxy-α-D-glucopyranoside. The starting point is a methylene with diastereotopic protons at 3.07 and 3.38 ppm (C at 54.9 ppm), the correlations of which (in COSY, TOCSY, and HSQC spectra) allow a spin system to be gathered formed by oxygenated methynes (H/C pairs: 4.05/70.9 3.26/75.4,

DOI: 10.1021/acs.jafc.6b02615
J. Agric. Food Chem. 2016, 64, 6708−6715

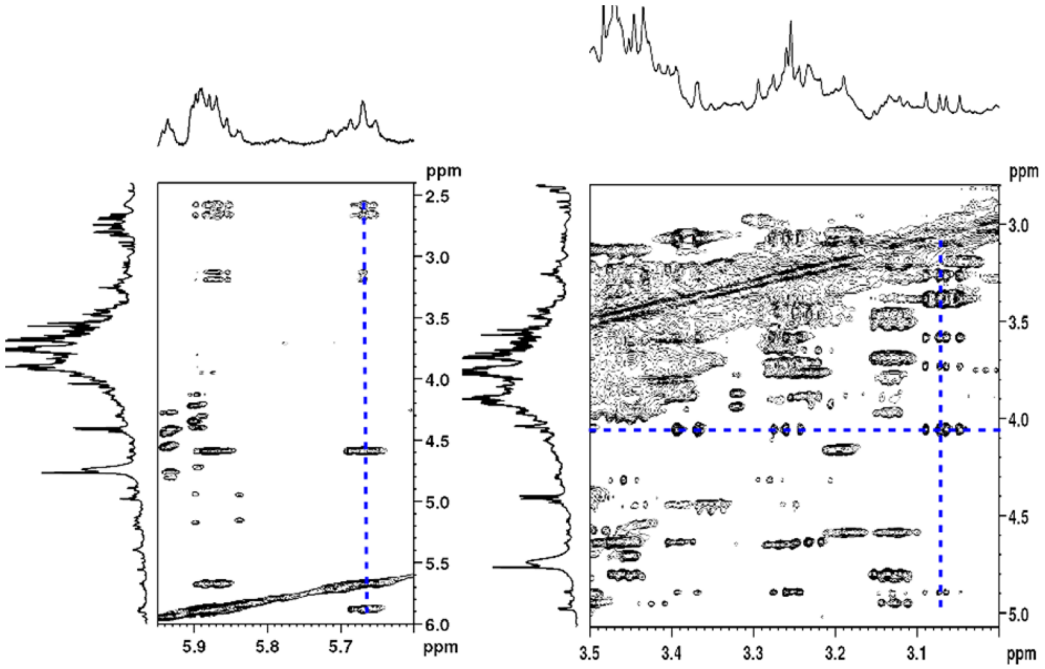

Figure 4. Partial TOCSY spectrum of Klamath alga suspension in D_2O evidencing signals of DhLys (left) and ADG (right).

3.73/75.7, 3.58/74.4), terminating with an α-anomeric proton at 4.89 ppm (C at 101.1 ppm). The HSQC-TOCSY experiment (Figure S2b,d) confirms the assignments. The anomeric proton at 4.89 ppm correlates, in the HMBC spectrum, with a carbon at 71.7 ppm, not belonging to the amino sugar ring, and gives ROE peaks with protons at 3.58 ppm (its vicinal one) and 3.45, 3.94 ppm. These last two protons belong to a methylene group (the carbon of which resonates at 71.7 ppm, Figure S3a) that gives HMBC correlations with carbons at 101.1 (bound to the proton resonating at 4.89 ppm), 73.6 (methyne), and 65.5 ppm (methylene). There is no unambiguous one-bond proton−carbon correlation (in the HSQC spectrum) for carbons at 73.6 and 65.5 ppm. These findings point to a glyceryl 6-amino-6-deoxy-α-D-glucopyranoside (ADG). The proton (shifted by 0.3−0.5 ppm due to the different solvents employed) and carbon chemical shifts (within 0−3 ppm) parallel those reported for the 6-amino-6-deoxy ring of ishigoside, a glyceroglycolipid isolated from the brown alga *Ishige okamurae*, with radical-scavenging properties.[33] This seems to us another interesting finding, for it indicates the presence of glycerol 6-amino-6-deoxy glucosides in AFA. Nevertheless, we did not identify, through ESI-QTOF mass analysis, adducts related to ADG (see ESI-QTOF Experiments); hence, we cannot exclude a further functionalization of this moiety at the amino group.

The second spin system is even more unusual and corresponds to DhLys. This spin system can be identified starting, for instance, from the doublet at 4.59 ppm (C at 54.7 ppm), which gives a COSY cross-peak with a triplet at 5.66 ppm and TOCSY cross-peaks with protons at 5.88, 5.66, 2.58, 2.66, 3.13, and 3.19 ppm. The last four belong to methylene groups, the carbons of which are found at 28.2 and 41.4 ppm, respectively. The presence of a double bond on the backbone of the fragment is confirmed by the chemical shifts of carbons bound to 5.66 and 5.88 ppm protons (128.1 and 135.1 ppm, respectively), and the *cis* configuration of the double bond is derived by the coupling constant (about 10 Hz) between the two ethylenic protons and a clear ROE between 4.59 and 2.58, 2.66 ppm signals. This spectral picture is confirmed by HSQC-TOCSY correlations (Figure S3c). No inter-residue ROEs were detected for DhLys and, in this case, a mass peak corresponding to the protonated molecule $[M + H]^+$ was found in ESI-QTOF spectra, confirming the presence of this molecule. Nevertheless, DhLys appears to be quite puzzling, for usually *trans*-3,4-DhLys moiety is found in important anticancer bioactive compounds, such as syringolin A (SylA). Syl A has been identified as a virulence factor, which irreversibly inhibits the 20S proteasome through a covalent mechanism.[34] Proteasome inhibitors, such as the clinically used anticancer agent bortezomib, represent a powerful class of chemotherapeutics.[35] Syls are a family (Syl A−F) of natural products formed by 12-membered macrolactams produced by strains of *Pseudomonas syringae*. The targeted search of protonated molecule or other adducts of Syls A, D, and F (those containing *trans*-DhLys) within ESI-QTOF mass spectral data did not give any result. Hence, we cannot derive a correlation between the presence of *cis*-3,4-DhLys and Syls in AFA.

A final comment is needed on the aromatic region of the proton spectrum (Figure 1), characterized by resonances mainly due to nucleobase derivatives (Table S1). Signals from alkyl-substituted phenyl rings were found, as confirmed by the HSQC experiment that displays correlations between proton (between 7.4 and 7.2 ppm) and carbon (between 133 and 130 ppm) signals. Nevertheless, we cannot relate these resonances to free phenylethylamine, because its aliphatic signals were not clearly detected.

High-performance liquid chromatography ESI-QTOF-MS was employed, operating in both positive and negative ionization modes, to confirm the presence of the metabolites detected through NMR analysis. The ESI-QTOF-MS (positive ion mode) gave a very complex total ion current chromatogram. The metabolites GalpG, Shi, and P334 eluted within the first 2 min and gave the highest contribution to the total ion current to peaks at 1.5, 1.8, and 2.0 min. The DhLys peak coeluted with other ions at 1.3 min. DhLys, P334, and Shi were detected as the protonated molecule $[M + H]^+$, whereas GalpG

DOI: 10.1021/acs.jafc.6b02615
J. Agric. Food Chem. 2016, 64, 6708−6715

was detected as a mixture of the protonated molecule $[M + H]^+$ and ammonium adduct $[M + NH_4]^+$.

In addition, in ESI-QTOF-MS negative ion mode experiments the metabolites were detected as $[M - H]^-$ ions, whereas GalpG was also detected as a formate adduct $[M + HCOO]^-$ at m/z 299.

Low-energy CID MS/MS spectra of Shi and P334 (Figure S4) parallel those reported by other authors,[36] whereas the GalpG CID spectrum in negative mode (Figure S5) is similar to that reported for its α-isomer by Chen et al.[37] The formulas that best fit the experimental isotopic peak intensity ratios of molecular species were $C_{14}H_{22}N_2O_8$ and $C_{13}H_{20}N_2O_8$ for P334 and Shi, respectively.

In the case of GalpG, the isotopic cluster of the protonated molecule and of the ammonium adduct suffer from peak overlapping with other species in all of the MS spectra acquired. Hence, we checked the isotopic peak intensity ratio of the product ion $[M - H]^-$ cluster at m/z 253, obtained from the product ion scan of the formate adduct $[M + HCOO]^-$ at m/z 299. The formula that best fits experimental intensities is $C_9H_{18}O_8$. We were not able to check the isotopic cluster intensities of the m/z 145 DhLys peak, for it suffers from severe overlapping in all MS spectra, and we did not find other molecular species other than $[M + H]^+$ and $[M - H]^-$ (Figure S6).

As for ADG, we did not come to an unambiguous structural assignment through MS/MS spectra. We searched the product ion scans for neutral losses of amino sugars (m/z 179) or of their dehydrated forms (m/z 161) and for product ions corresponding to protonated amino sugars (m/z 180) or protonated dehydrated amino sugars (m/z 162). A possible species containing the 6-amino-6-deoxy-α-D-glucopyranosyl fragment could be the m/z 455 ion (Figure S7) that displays a m/z 179 neutral loss and shows product ions at m/z 162 and 180. The remaining ions, in particular those at m/z 84, 126, 138, 144, 168, 186, and 276, are the same reported for the fragmentation of *N*-acetylmuramic acid. Our data suggest that the m/z 455 ion could derive from *N*-acetylmuramic acid, or an isomer of it, bound to an amino sugar. *N*-Acetylmuramic acid is usually bound to *N*-acetylglucosamine in bacterial cells, and it has been reported that cell walls of blue-green algae possess a mucopolymer similar to that of bacterial cell walls.[38] Thus, we hypothesize that ADG could be involved in the structure of such a mucopolymer.

Summarizing, we showed that high-resolution NMR spectroscopy applied to AFA powder suspensions reveals a very complex metabolic profile. Resonances from small metabolites, overlapped to a background due to signals from high molecular weight polysaccharides, were detected. Apart from free and bound amino acids and monosaccharides, the most interesting metabolites found are two MAAs, that is, P334 and Shi, two glycopyranosides, that is, GalpG, and ADG, and *cis*-3,4-DhLys. All of these molecules possess known nutraceutical properties and high biological activity. The presence of *cis*-3,4-DhLys was revealed for the first time, even though we were not able to find a direct connection to Syls production.

NMR findings were checked by ESI-QTOF-MS that confirmed most of them, leaving the complete structure of the ADG derivative still an open question.

Although this study proves the value of the application of NMR spectroscopy directly on complex mixtures and supports the use of NMR to monitor valuable metabolites, such as P334 and Shi, directly of AFA powder suspensions, further investigations are necessary to gain a deeper insight into the very complex AFA metabolome.

■ ASSOCIATED CONTENT

Supporting Information

The Supporting Information is available free of charge on the ACS Publications website at DOI: 10.1021/acs.jafc.6b02615.

Selected regions of HSQC-TOCSY, HSQC spectra, and low-energy CID MS/MS spectra as well as further NMR data for metabolites found in AFA (PDF)

■ AUTHOR INFORMATION

Corresponding Author

*(A.M.) Phone: +39 059 2058636. E-mail: adele.mucci@unimore.it.

Funding

Fondazione Cassa di Risparmio di Modena and Centro Interdipartimentale Grandi Strumenti of the University of Modena and Reggio Emilia are greatly acknowledged for financial support in the acquisition of the Bruker Avance III HD 600 spectrometer.

Notes

The authors declare no competing financial interest.

■ ABBREVIATIONS USED

Ac, acetate; ADG, glyceryl 6-amino-6-deoxy-α-D-glucopyranoside; AFA, *Aphanizomenon flos-aquae*; Ala, alanine; Asp, aspartate; CID MS/MS, low-energy collision-induced dissociation tandem mass spectrometry; COSY, correlation spectroscopy; DhLys, dehydrolysine; ESI, electrospray ionization; GalpG, glyceryl β-D-galactopyranoside; Glc, glucose; Gln, glutamine; Glu, glutamate; HMBC, heteronuclear multiple-bond correlation; HR-MAS, high-resolution magic angle spinning; HSQC, heteronuclear single-quantum coherence; Lac, lactate; MAAs, mycosporine-like amino acids; MAO, monoamine oxidase; MS, mass spectrometry; NMR, nuclear magnetic resonance; NOESY, nuclear Overhauser effect spectroscopy; P334, porphyra-334; QTOF, quadrupole-time-of-flight; ROESY, rotating Overhauser effect spectroscopy; Shi, shinorine; Syl, syringolin; Thr, threonine; TOCSY, total correlation spectroscopy

■ REFERENCES

(1) Baroni, L.; Scoglio, S.; Benedetti, S.; Bonetto, C.; Pagliarani, S.; Benedetti, Y.; Rocchi, M.; Canestrari, F. Effect of a Klamath algae product ("AFA-B12") on blood levels of vitamin B12 and homocysteine in vegan subjects: a pilot study. *Int. J. Vitam. Nutr. Res.* **2009**, *79*, 117−123.

(2) Hart, A. N.; Zaske, L. A.; Patterson, K. M.; Drapeau, C.; Jensen, G. S. Natural killer cell activation and modulation of chemokine receptor profile in vitro by an extract from the cyanophyta *Aphanizomenon flos-aquae*. *J. Med. Food* **2007**, *10*, 435−441.

(3) Pugh, N.; Pasco, D. S. Characterization of human monocyte activation by a hydrosoluble preparation of *Aphanizomenon flos-aquae*. *Phytomedicine* **2001**, *8*, 445−453.

(4) Scoglio, S.; Benedetti, S.; Canino, C.; Santagni, S.; Rattighieri, E.; Chierchia, E.; Canestrari, F.; Genazzani, D. A. Effect of a 2-month treatment with Klamin®, a Klamath algae extract, on the general well-being, antioxidant profile and oxidative status of postmenopausal women. *Gynecol. Endocrinol.* **2009**, *25*, 235−240.

(5) Scoglio, S.; Benedetti, Y.; Benvenuti, F.; Battistelli, S.; Canestrari, F.; Benedetti, S. Selective monoamine oxidase B inhibition by an *Aphanizomenon flos-aquae* extract and by its constitutive active

DOI: 10.1021/acs.jafc.6b02615
J. Agric. Food Chem. 2016, 64, 6708−6715

principles phycocyanin and mycosporine-like amino acids. *Phytomedicine* **2014**, *21*, 992−997.
(6) Benedetti, S.; Benvenuti, F.; Pagliarani, S.; Francogli, S.; Scoglio, S.; Canestrari, F. Antioxidant properties of a novel phycocyanin extract from the blue-green alga *Aphanizomenon flos-aquae*. *Life Sci.* **2004**, *75*, 2353−2362.
(7) Benedetti, S.; Benvenuti, F.; Scoglio, S.; Canestrari, F. Oxygen radical absorbance capacity of phycocyanin and phycocyanobilin from the food supplement *Aphanizomenon flos-aquae*. *J. Med. Food* **2010**, *13*, 223−227.
(8) Gilroy, D. J.; Kauffman, K. W.; Hall, R. A.; Huang, X.; Chu, F. S. Assessing potential health risks from microcystin toxins in blue-green algae dietary supplements. *Environ. Health Perspect.* **2000**, *108*, 435−439.
(9) Kusaga, A. Decreased β-phenylethylamine in urine of children with attention deficit hyperactivity disorder and autistic disorder. *No To Hattatsu* **2002**, *34*, 243−248.
(10) Kusaga, A.; Yamashita, Y.; Koeda, T.; Hiratani, M.; Kaneko, M.; Yamada, S.; Matsuishi, T. Increased urine phenylethylamine after methylphenidate treatment in children with ADHD. *Ann. Neurol.* **2002**, *52*, 372−374.
(11) Sedriep, S.; Xia, X.; Marotta, F.; Zhou, L.; Yadav, H.; Yang, H.; Soresi, V.; Catanzaro, R.; Zhong, K.; Polimeni, A.; Chui, D. H. Beneficial nutraceutical modulation of cerebral erythropoietin expression and oxidative stress: an experimental study. *J. Biol. Regul. Homeos. Agents* **2011**, *25*, 187−194.
(12) Shytle, D. R.; Tan, J.; Ehrhart, J.; Smith, A. J.; Sanberg, C. D.; Sanberg, P. R.; Anderson, J.; Bickford, P. C. Effects of blue-green algae extracts on the proliferation of human adult stem cells in vitro: a preliminary study. *Med. Sci. Monit.* **2010**, *16*, 1−5.
(13) Bhat, V. B.; Madyastha, K. M. C-phycocyanin: a potent peroxyl radical scavenger in vivo and in vitro. *Biochem. Biophys. Res. Commun.* **2000**, *275*, 20−25.
(14) Bhat, V. B.; Madyastha, K. M. Scavenging of peroxynitrite by phycocyanin and phycocyanobilin from *Spirulina platensis*: protection against oxidative damage to DNA. *Biochem. Biophys. Res. Commun.* **2001**, *285*, 262−266.
(15) Romay, C.; Gonzalez, R. Phycocyanin is an antioxidant protector of human erythrocytes against lysis by peroxyl radicals. *J. Pharm. Pharmacol.* **2000**, *52*, 367−368.
(16) Romay, C.; Armesto, J.; Remirez, D.; Gonzalez, R.; Ledon, N.; Garcia, I. Antioxidant and anti-inflammatory properties of C-phycocyanin from blue-green algae. *Inflammation Res.* **1998**, *47*, 36−41.
(17) Reddy, C. M.; Bhat, V. B.; Kiranmai, G.; Reddy, M. N.; Reddanna, P.; Madyastha, K. M. Selective inhibition of cyclooxygenase-2 by C-phycocyanin, a biliprotein from *Spirulina platensis*. *Biochem. Biophys. Res. Commun.* **2000**, *277*, 599−603.
(18) Torres, A.; Enk, C. D.; Hochberg, M.; Srebnik, M. Porphyra-334, a potential natural source for UVA protective sunscreens. *Photochem. Photobiol. Sci.* **2006**, *5*, 432−435.
(19) Scoglio, S.; Canestrari, F.; Benedetti, S.; Benedetti, Y.; Delgado-Esteban, M. Aphanizomenon flos aquae preparation, extracts and purified components thereof for the treatment of neurological, neurodegenerative and mood disorders. WO 2008000430, 2008, A2.
(20) Choi, Y.-H.; Yang, D. J.; Kulkarni, A.; Moh, S. H.; Kim, K. W. Mycosporine-like amino acids promote wound healing through focal adhesion kinase (FAK) and mitogen-activated protein kinases (MAP kinases) signaling pathway in keratinocytes. *Mar. Drugs* **2015**, *13*, 7055−7066.
(21) Abd El-Baky, H. H.; El Baz, F. K.; El-Baroty, G. S. Characterization of nutraceutical compounds in blue green alga *Spirulina maxima*. *J. Med. Plants Res.* **2008**, *2*, 292−300.
(22) Benedetti, S.; Rinalducci, S.; Benvenuti, F.; Francogli, S.; Pagliarani, S.; Giorgi, L.; Micheloni, M.; D'Amici, G. M.; Zolla, L.; Canestrari, F. Purification and characterization of phycocyanin from the blue-green alga *Aphanizomenon flos-aquae*. *J. Chromatogr. B: Anal. Technol. Biomed. Life Sci.* **2006**, *833*, 12−18.
(23) Evans, A. M.; Li, D.; Jones, A.; Games, M. P.; Games, D. E.; Gallon, J. R.; Walton, T. J. Analysis by gas chromatography-mass spectrometry of the fatty acid composition during temperature adaptation in *Aphanizomenon flos-aquae*, a diazotrophic cyanobacterium from the Baltic Sea. *Biochem. Soc. Trans.* **1996**, *24*, 475S.
(24) Abd El-Bakya, H. H.; El-Baroty, G. S. Characterization and bioactivity of phycocyanin isolated from *Spirulina maxima* grown under salt stress. *Food Funct.* **2012**, *3*, 381−388.
(25) Mendiola, J. A.; Marn, F. R.; Hernndez, F. S.; Arredondo, O. B.; Seorns, F. J.; Ibaez, E.; Reglero, G. Characterization via liquid chromatography coupled to diode array detector and tandem mass spectrometry of supercritical fluid antioxidant extracts of *Spirulina platensis* microalga. *J. Sep. Sci.* **2005**, *28*, 1031−1038.
(26) Mucci, A.; Parenti, F.; Righi, V.; Schenetti, L. Citron and lemon under the lens of HR-MAS NMR spectroscopy. *Food Chem.* **2013**, *141*, 3167−3176.
(27) Righi, V.; Parenti, F.; Tugnoli, V.; Schenetti, L.; Mucci, A. *Crocus sativus* petals: waste or valuable resource? The answer of high-resolution and high-resolution magic angle spinning nuclear magnetic resonance. *J. Agric. Food Chem.* **2015**, *63*, 8439−8444.
(28) Neuhaus, D.; Williamson, M. P. *The Nuclear Overhauser Effect in Structural and Conformational Analysis*, 2nd ed.; Wiley-VCH: New York, 2000.
(29) Klisch, M.; Richter, P.; Puchta, R.; Donat-P. Häder, D.-P.; Bauer, W. The stereostructure of porphyra-334: an experimental and calculational NMR investigation. Evidence for an efficient 'proton sponge'. *Helv. Chim. Acta* **2007**, *90*, 488−511.
(30) Carignan, M. O.; Carreto, J. I. Characterization of mycosporine-serine-glycine methyl ester, a major mycosporine-like amino acid from dinoflagellates: a mass spectrometry study. *J. Phycol.* **2013**, *49*, 680−688.
(31) Broberg, A.; Kenne, L. Use of high-resolution magic angle spinning nuclear magnetic resonance spectroscopy for in situ studies of low-molecular-mass compounds in red algae. *Anal. Biochem.* **2000**, *284*, 367−374.
(32) Zhang, J.; Li, C.; Yu, G.; Guan, H. Total synthesis and structure-activity relationship of glycoglycerolipids from marine organisms. *Mar. Drugs* **2014**, *12*, 3634−3659.
(33) Zou, Y.; Li, Y.; Kim, M.-M.; Lee, S.-H.; Kim, S.-H. Ishigoside, a new glyceroglycolipid isolated from the brown alga *Ishige okamurae*. *Biotechnol. Bioprocess Eng.* **2009**, *14*, 20−26.
(34) Groll, M.; Schellenberg, B.; Bachmann, A. S.; Archer, C. R.; Huber, R.; Powell, T. K.; Lindow, S.; Kaiser, M.; Dudler, R. A plant pathogen virulence factor inhibits the eukaryotic proteasome by a novel mechanism. *Nature* **2008**, *452*, 755−758.
(35) Groll, M.; Berkers, C. R.; Ploegh, H. L.; Ovaa, H. Crystal structure of the boronic acid-based proteasome inhibitor bortezomib in complex with the yeast 20S proteasome. *Structure* **2006**, *14*, 451−456.
(36) Roullier, C.; Chollet-Krugler, M.; Pferschy-Wenzig, E.-M.; Maillard, A.; Rechberger, G. N.; Legouin-Gargadennec, B.; Bauer, R.; Boustie, J. Characterization and identification of mycosporines-like compounds in cyanolichens. Isolation of mycosporine hydroxyglutamicol from *Nephroma laevigatum* Ach. *Phytochemistry* **2011**, *72*, 1348−1357.
(37) Chen, J.; Song, D.; Luo, Q.; Mou, T.; Yang, R.; Chen, H.; He, S.; Yan, X. Determination of floridoside and isofloridoside in red algae by high-performance liquid chromatography tandem mass spectrometry. *Anal. Lett.* **2014**, *47*, 2307−2316.
(38) Drews, G.; Meyer, H. Chemical composition of cell walls of *Anacystis nidulans* and *Chlorogloea fritschii*. *Arch. Microbiol.* **1964**, *48*, 259−267.

DOI: 10.1021/acs.jafc.6b02615
J. Agric. Food Chem. 2016, 64, 6708−6715